Comparison study between brick and ribbed dome by using F. E. analysis

Cite as: AIP Conference Proceedings **2660**, 020051 (2022); https://doi.org/10.1063/5.0108468
Published Online: 17 November 2022

S. Kh Faleh, I. S. Saleh and A. H. Chkheiwer

Comparison Study Between Brick and Ribbed Dome by Using F. E. Analysis

S Kh Faleh[1a)], I S Saleh[1b)] and A H Chkheiwer[1c)]

[1]*University of Basrah /Engineering College /Civil Eng. Department, Basrah, Iraq.*

[a)]Corresponding author: saddam.faleh@uobasrah.edu.iq
[b)] ihab.sabri@uobasrah.edu.iq
[c)]aqeel.chkeiwer@uobasrah.edu.iq

Abstract. Engineers are particularly interested in brick due to the fact that they contain a maximum amount of space with a minimum amount of surface area, they have shown to be very inexpensive in terms of constructional materials consumption The first braced dome was the ribbed dome. As the name implies, it is made up of a sequence of similar meridional solid girders or trusses, which are linked at the crown by an elastic band or a compression band. In this paper a comparison between the strains and deformations of a brick dome and that of a ribbed dome. With the help of STAAD Pro V8i, finite element models of these domes were built and analyzed. For the bricks, shell elements were used, while steel sections were used for the ribs and rings. There was a pressure on the entire surface of the dome from the loads. Brick failure criteria were determined by analyzing stresses and deflections of the dome. Various distributions of ribs and rings were tested in order to determine the optimal angle of rib distribution and ring spacing. The stresses and deformations of a brick dome and a ribbed dome were compared in this paper. STAAD Pro V8i software was used to create and analyze finite element models of these domes. Shell elements were used to simulate bricks, while steel sections were used to simulate ribs and rings. Loads were applied as a pressure on the entire dome's surface. The stresses and deflections of the dome were investigated in order to determine the failure criteria in bricks. In order to identify the optimal angle of the steel rib distribution and the space between rings, ribbed domes with various steel rib and ring distributions were tested. In order to compare the brick dome with ribbed dome, new analysis of the same dimensions of brick dome were done. Standards steel section was used for ribs and rings, 240 mm thickness of brick fill the area between ribs and rings. The behavior of this dome under the same load was study. The analysis showed, that dome with steel ribs of angle in plan theta (15 degree) was successful to resist the loads and the tensile stresses of brick were less than 0.20 N/mm^2 (maximum tensile strength of used brick), when the angle in plane theta increase to 22.5 and 30 degrees, the hoop tensile stresses in brick exceeds the tensile strength limit. So that the meridional cracks may be appear at the springing zone of dome. While crushing failure did not occur, where the compressive stresses in all models were lower as compared with brick allowable compressive strength (0.80 N/mm^2).

INTRODUTION

A Dome (Latin: "Domus" Meaning "House") [1]. Domes have a long architectural history dating back to prehistory, and they are now used in a variety of fields including construction, houses, Shrines, Mosques, palaces, administrative buildings, naval construction, and many others. Dome's construction has developed gradually from mud, brick, and stone to reinforced concrete and ribbed steel domes with various shapes and construction technique.

These thin shells resemble revolution surfaces and are used to create domes. There must be a thickness (t) of less than 4.5 % of the radius R to ensure that the thrust line remains inside of the brickwork and that forces are not deformed or unbalanced. There is a dramatic reduction in the minimum thickness required when the dome is not fully encircled by 180 degrees [2].

As new production techniques allowed predicted iron and wrought iron to be manufactured in greater quantities and at lower prices during the industrial revolution, braced steel domes have grown increasingly popular in recent years [3].

4th International Conference on Materials Engineering & Science
AIP Conf. Proc. 2660, 020051-1–020051-14; https://doi.org/10.1063/5.0108468
Published by AIP Publishing. 978-0-7354-4275-7/$30.00

To compare the behavior of brick domes with constant and varied thicknesses to ribbed dome behavior, this article was written. "As far as braced domes are concerned, the ribbed dome is the oldest one. At the crown, compression rings connect a sequence of similar meridional solid beams. As the ribs are connected by concentric rings, they form trapezium-shaped grids. A steel or reinforced concrete tension ring stiffens the base of the ribbed dome." [4].

In the study of brick dome, constant thicknesses of 240 mm, and 600, also variable stepped thickness of 600mm to 240 mm were used. While in analysis of ribbed dome different number of intersecting "ribs" and "rings", A "ribs" are a group of elements that lie a long a meridian (longitude) line and “rings” are a group of elements that constitute a horizontal circle hoop (latitude) line, the mesh is filled by a 240 mm constant thickness brick. Because it lacks a diagonal element, in order to be structurally sound, ribbed domes must be joined together securely [5].

GOAL OF THE RESEARCH

Analytic formulations for existing pointed dome are studied, as well as a comparison between masonry traditional method of construction with steel-ribbed dome filled with brick are investigated with determining the response of dome such as stresses and deformations under same loading case. Thus, there is an exploration to the best construction method for large span domes to behave safe with minimum deformations.

GEOMETRIC PARAMETER OF DOME

In this paper specified type of large domes were studied, diameter of the dome (D) at base (drum) is 23.6 m, diameter of the dome (D) at springing is 24.94 m and total height (H) is 18 m as shown in Figure 1.

The dome has been analyzed as a brick dome with constant thickness of 240 mm (BD#1) and 600 mm (BD#2), also with stepped variable thickness 600 mm to 240 mm (BD#3), furthermore ribbed dome (RD) (steel ribs, rings and 240 mm thickness brick fills the areas between ribs and rings) with rigid joints were studied also.

In six cases, the ribbed dome had ribs 12, 16, and 24 uniformly placed along its circumference at angles theta (15, 22.5, and 30 degrees), respectively, in the simulations. Rings were separated into 1.5 m and 3 m sections along the vertex height of the dome for each number of ribs.

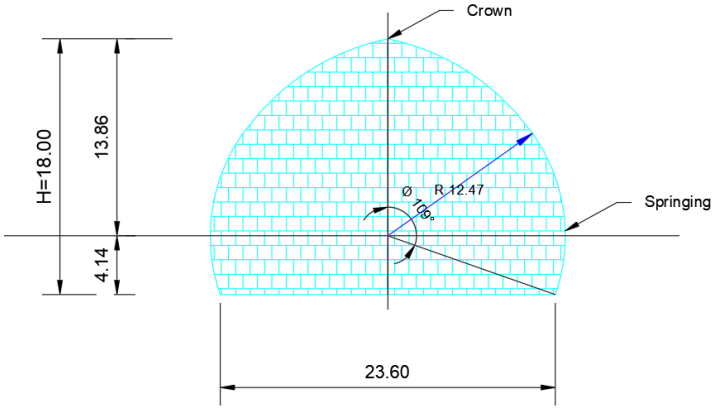

FIGURE 1. Shape and dimensions in meters of studied pointed dome

STRUCTURAL BEHAVIOR OF BRICK AND RIBBED DOMES

The same dome has been analyzed as a brick with 240 mm and 600 mm constant thickness, stepped (600 mm, 480 mm and 360 mm) for lower half height of dome and 240 mm thick for the remaining height, and ribbed dome (The "ribs" of a dome are the radial lines of Steel I-sections that extend from the crown down to the springing, and double CH-Sections rings around the ribs, and then the structure is filled with brick thickness 240 mm) to conduct a comparison of stresses and deformations. It is a frequent feature of unreinforced masonry domes that the bottom portion of the dome spreads outward under vertical loads due to thrust force. A meridional crack forms at the base of

the dome as a result of hoop tension stress, as seen in Figure 2 [2]. A similar pattern of cracking can be found in domes with tension rings, but they don't extend all that far, as can be shown in Figure 2.

In spite of the fact that a dome's stability may be maintained if fractures emerge due to masonry's intrinsic ductility [6], their proliferation will drastically weaken the dome. A large number of cracks in a structure can compromise its structural integrity, as demonstrated by the unforeseen collapse of a dome in Noto Cathedral [7].

In a dome, loads, including one's own weight, result in meridian and parallel stresses [8, 9, 10]. The meridian stresses are always compressions. Tensions in the lower dome and compressions in the upper dome are examples of parallel stresses (except for the typical case of domes with flat crown and heavy lantern). The highest parallel tension stress is commonly found at the springing, and it often surpasses the masonry tension strength even when the load is not applied to the masonry structure. For this reason, that many masonry domes are damaged quickly after completion (sometimes during the construction). Cracking begins at the springing and continues to extend vertically downhill through the rotor and upward toward the crest, sometimes stopping at the haunches and other times reaching the crown structure) [9].

Until the brickwork cracks, parallel tension pressures exist. Consequently, vertical cracking reduces the dome's size from two to one. The brick dome is merely a shell from an architectural aspect, but it is a structural system of arches because of the abundance of vertical fissures in the dome. Dimensional stability of masonry arches is affected by two parameters: thickness-to-span and lateral springing thrust [10]. Due to the fact that the fractured dome acts similarly to a brickwork arch, these two criteria determine the stability of masonry domes. Due to vertical cracking, the thickness of a masonry dome is that of the arches it splits into. As a result, the thickness-to-span ratio (first parameters) does not refer to the thickness of the shell, but rather to the shape of the curved elements into which the shell divides. The abutment in a masonry dome corresponds with a block into which the drum is split due to vertical cracking. As a result, the lateral springing thrust (second parameters) is the horizontal thrust transmitted by the cracked dome to the cracked drum via the lowest latitude parallel. Any masonry arch must have a minimum thickness-to-span ratio [10]. As a result, a masonry dome is only stable if the thickness of the arches into which it splits is greater than the minimum thickness for the span.

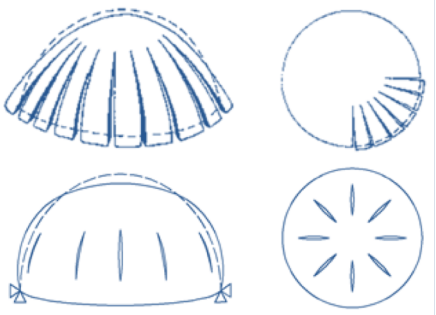

FIGURE 2. Spherical masonry domes with and without tension ring [2]

MATERIALS PROPERTIES OF DOME

In model simulation class B Iraqi bricks were used [11], I- section steel ribs and double channel steel rings according to British standards [12]. Table 1 shows the brick properties.

Modulus of Elasticity of clay masonry and steel is found according to uniform building code [13]

Modulus of elasticity of clay masonry;

$$E_m = 750\, f'_m \tag{1}$$

Modulus of rigidity (Shear modulus) of clay masonry;

$$G = 0.4\ Em \tag{2}$$

Modulus of elasticity of steel;

$$Es = 200 * 10^3\ MPa \tag{3}$$

Yield strength of steel;

$$fy = 275 \text{ MPa} \quad (4)$$

TABLE 1. Dome brick properties [13]

Modulus of Elasticity (E_m) MPa	Modulus of rigidity (G) MPa	Poisson's Ratio (ν)	Density (γ) (kN/m^3)	compressive strength (f'_m) MPa	Allowable compressive strength (f_c) MPa	Allowable tensile strength (f_t) MPa
9000	3600	0.15	18	13	0.80	0.20

LOADING

A- LOAD COMBINATION

The load magnitude and combination which used in this study is according to American society of civil engineers [14], which is defined as follows:

$$1.2\ D + 1.6\ Lr \quad (5)$$

D = dead load, total weight of the brick and finishing.
L_r = roof live load, 0.96 kN/m^2 for pitched and curved roofs***.**

***Reduction in roof live loads [14]**

For flat, pitched, and curved roofs the American society for civil engineers are permitted to be designed for a reduced roof live load as shown in the following equation;

$$Lr = Lo\ R1\ R2 \quad (6)$$

Where $0.58 \leq L_r \leq 0.96$

R_1 = 1 for $A_t \leq 18.58$ m^2
$R_1 = 1.2 - 0.011\ A_t$ for $18.58\ m^2 < A_t < 55.74\ m^2$
0.6 for $A_t \geq 55.74$ m^2

Where A_t = tributary area in (m^2) supported by any structural member and,

R_2 = 1 for $F \leq 4$
$R_2 = 1.2 - 0.05\ F$ for $4 < F < 12$
0.6 for $F \geq 12$

Where for an arch or dome F = rise-to-span ratio multiplied by 32.
So that L_r = 0.60 kN/m^2 roof live load used in study.

These are commonly defined dead and live load conditions on the dome as a vertical and symmetrical load.

B- LOAD SIMULATION

The loadings were calculated partially manually and rest was generated using STAAD Pro V8i. Software. The loading cases were categorized as; Self-weigh of brick, dead load from finishing, and roof live load. The critical combination of loads has been represented according to equation (5).

STRUCTURAL MODEL RESULTS AND DISCUSSIONS

All | Summary

	Node	L/C	Horizontal X mm	Vertical Y mm	Horizontal Z mm	Resultant mm
Max X	6	3 1.2DL+1.6L	**0.908**	-0.489	-0.000	1.032
Min X	2583	3 1.2DL+1.6L	**-0.908**	-0.489	0.000	1.032
Max Y	1127	3 1.2DL+1.6L	-0.000	**-0.000**	0.000	0.000
Min Y	5423	3 1.2DL+1.6L	-0.060	**-1.472**	-0.016	1.473
Max Z	3927	3 1.2DL+1.6L	0.000	-0.489	**0.908**	1.032
Min Z	1239	3 1.2DL+1.6L	-0.000	-0.489	**-0.908**	1.032
Max rX	3923	3 1.2DL+1.6L	0.000	-0.217	0.383	0.440
Min rX	1235	3 1.2DL+1.6L	-0.000	-0.217	-0.383	0.440
Max rY	5679	3 1.2DL+1.6L	0.601	-0.333	-0.297	0.749
Min rY	7885	3 1.2DL+1.6L	-0.555	-0.596	0.371	0.895
Max rZ	2579	3 1.2DL+1.6L	-0.383	-0.217	0.000	0.440
Min rZ	2	3 1.2DL+1.6L	0.383	-0.217	-0.000	0.440
Max Rst	5423	3 1.2DL+1.6L	-0.060	-1.472	-0.016	**1.473**

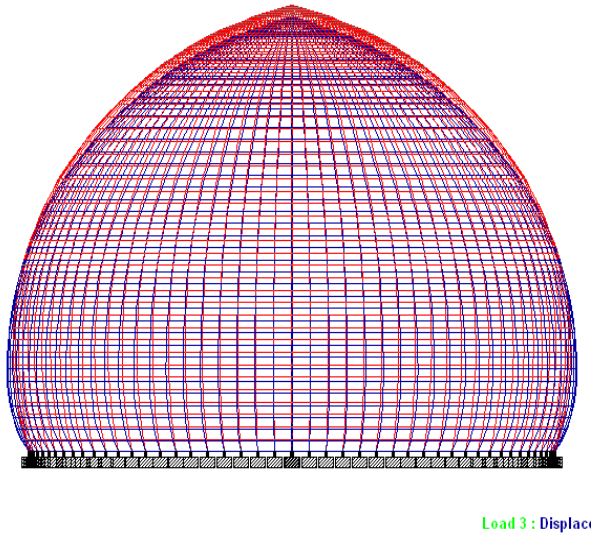

FIGURE 3. Deflection Shape and maximum deflection results of BD#1

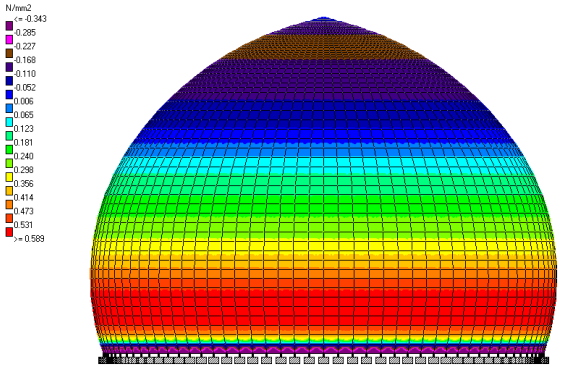

FIGURE4. Hoop Stresses of BD#1

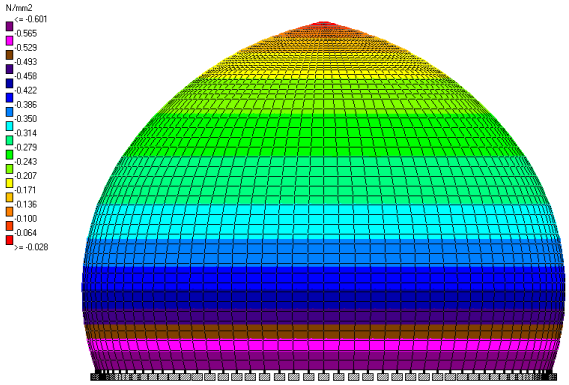

FIGURE 5. Meridional Stresses of BD#1

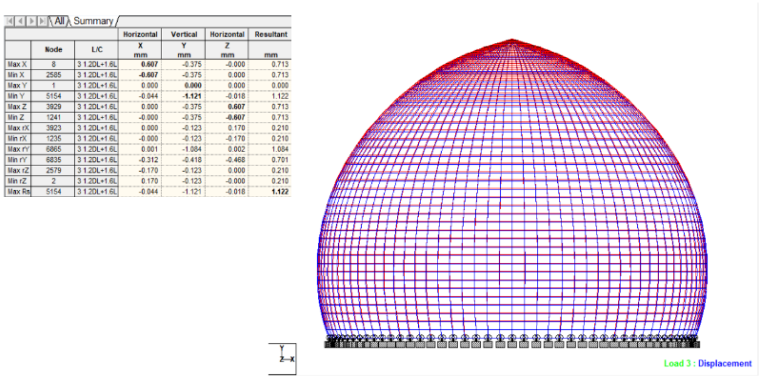

FIGURE 6. Deflection Shape and maximum deflection of BD#2

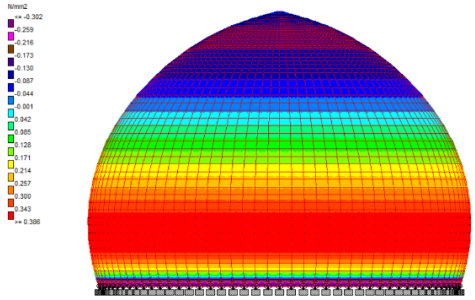

FIGURE 7. Hoop Stresses of BD#2

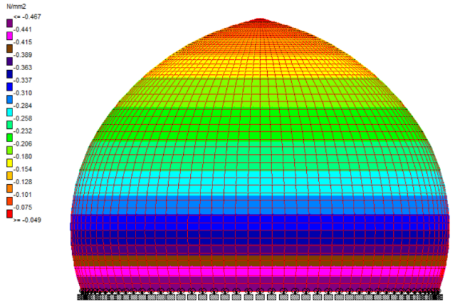

FIGURE 8. Meridional Stresses of BD#2

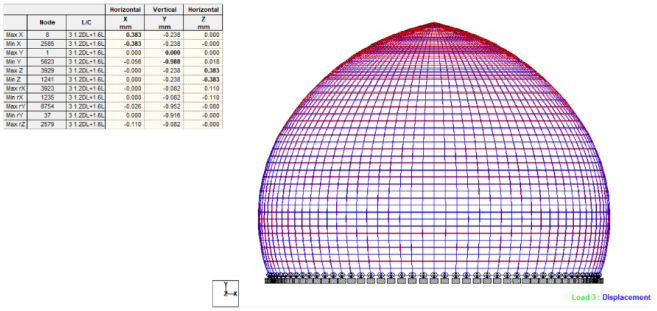

FIGURE 9. Deflection Shape and maximum deflection results of BD#3

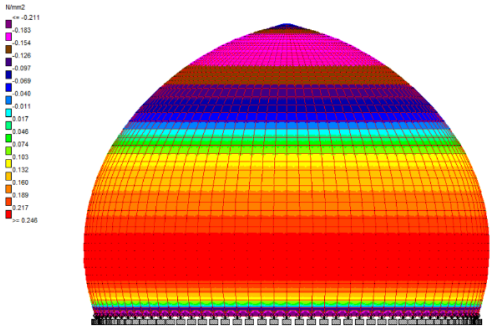

FIGURE 10. Hoop Stresses of BD#3

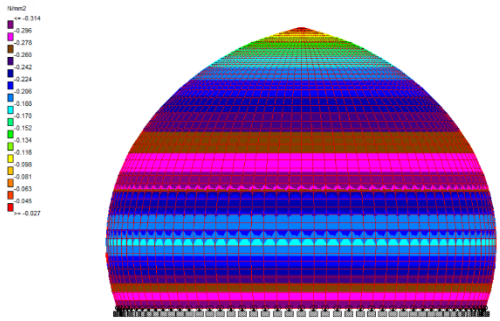

FIGURE 11. Meridional Stresses of BD#3

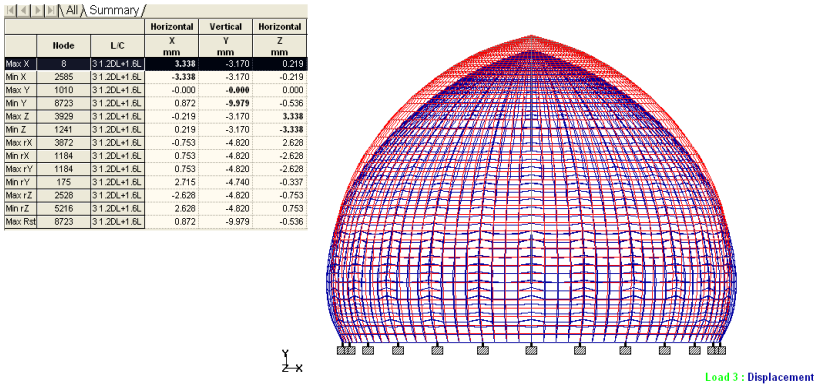

	Node	L/C	Horizontal X mm	Vertical Y mm	Horizontal Z mm
Max X	8	31 2DL+1.6L	**3.338**	-3.170	0.219
Min X	2585	31 2DL+1.6L	**-3.338**	-3.170	-0.219
Max Y	1010	31 2DL+1.6L	-0.000	**-0.000**	0.000
Min Y	8723	31 2DL+1.6L	0.872	**-9.979**	-0.536
Max Z	3929	31 2DL+1.6L	-0.219	-3.170	**3.338**
Min Z	1241	31 2DL+1.6L	0.219	-3.170	**-3.338**
Max rX	3872	31 2DL+1.6L	-0.753	-4.820	2.628
Min rX	1184	31 2DL+1.6L	0.753	-4.820	-2.628
Max rY	1184	31 2DL+1.6L	0.753	-4.820	-2.628
Min rY	175	31 2DL+1.6L	2.715	-4.740	-0.337
Max rZ	2528	31 2DL+1.6L	-2.628	-4.820	-0.753
Min rZ	5216	31 2DL+1.6L	2.628	-4.820	0.753
Max Rst	8723	31 2DL+1.6L	0.872	-9.979	-0.536

FIGURE 12. Deflection Shape and maximum deflection results of RD#1, having in plan theta angle 15° and rings spacing 1.5 m

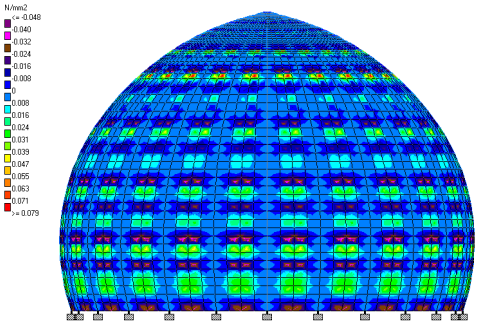

FIGURE 13. Hoop Stresses of RD#1, having in plan theta angle 15° and rings spacing 1.5 m

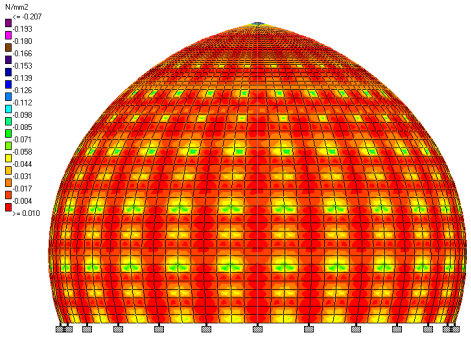

FIGURE 14. Meridional Stresses of RD#1, having in plan theta angle 15° and rings spacing 1.5 m

	Node	L/C	Horizontal X mm	Vertical Y mm	Horizontal Z mm	Resultant mm
Max X	123	31 2DL+1.6L	**4.794**	-3.490	-0.043	5.930
Min X	2811	31 2DL+1.6L	**-4.794**	-3.490	0.043	5.930
Max Y	1010	31 2DL+1.6L	-0.000	**-0.000**	0.000	0.000
Min Y	1377	31 2DL+1.6L	-1.728	**-10.660**	1.480	10.900
Max Z	4155	31 2DL+1.6L	0.043	-3.490	**4.794**	5.930
Min Z	1467	31 2DL+1.6L	-0.043	-3.490	**-4.794**	5.930
Max rX	3872	31 2DL+1.6L	-1.661	-4.623	2.995	5.754
Min rX	1184	31 2DL+1.6L	1.661	-4.623	-2.995	5.754
Max rY	4320	31 2DL+1.6L	0.060	-4.620	3.425	5.751
Min rY	175	31 2DL+1.6L	3.404	-4.505	0.360	5.657
Max rZ	2528	31 2DL+1.6L	-2.995	-4.623	-1.661	5.754
Min rZ	5216	31 2DL+1.6L	2.995	-4.623	1.661	5.754
Max Rst	1377	31 2DL+1.6L	-1.728	-10.660	1.480	**10.900**

FIGURE 15. Deflection Shape and maximum deflection results of RD#2, having in plan theta angle 15° and rings spacing 3.0 m

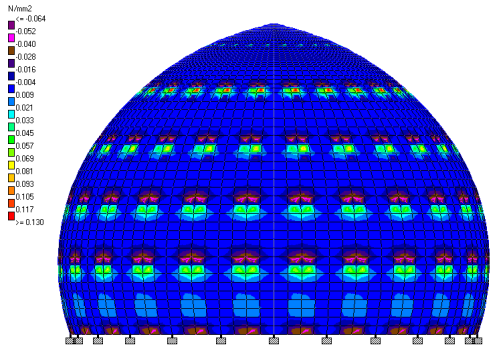

FIGURE 16. Hoop Stresses of RD#2, having in plan theta angle 15° and rings spacing 3.0 m

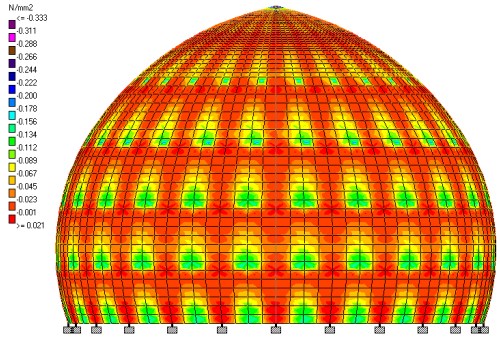

FIGURE 17. Meridional Stresses of RD#2, having in plan theta angle 15° and rings spacing 3.0 m

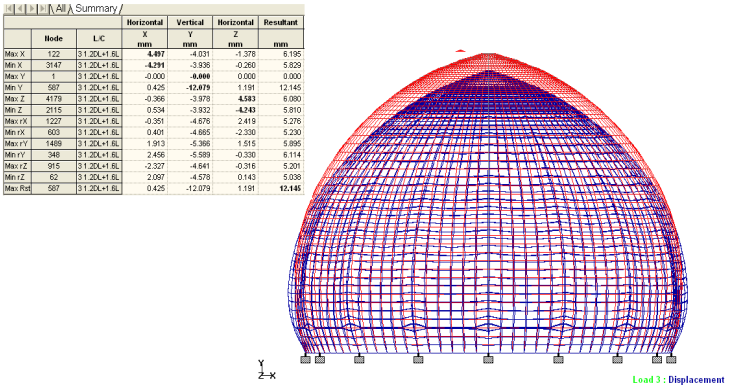

	Node	L/C	Horizontal X mm	Vertical Y mm	Horizontal Z mm	Resultant mm
Max X	122	31.2DL+1.6L	**4.497**	-4.031	-1.378	6.195
Min X	3147	31.2DL+1.6L	**-4.291**	-3.936	-0.260	5.829
Max Y	1	31.2DL+1.6L	-0.000	**-0.000**	0.000	0.000
Min Y	587	31.2DL+1.6L	0.425	**-12.079**	1.191	12.145
Max Z	4179	31.2DL+1.6L	-0.366	-3.978	**4.583**	6.080
Min Z	2115	31.2DL+1.6L	0.534	-3.832	**-4.243**	5.810
Max rX	1227	31.2DL+1.6L	-0.351	-4.578	2.419	5.276
Min rX	603	31.2DL+1.6L	0.401	-4.665	-2.330	5.230
Max rY	1489	31.2DL+1.6L	1.913	-5.366	1.515	5.895
Min rY	346	31.2DL+1.6L	2.456	-5.589	-0.330	6.114
Max rZ	915	31.2DL+1.6L	-2.327	-4.641	-0.316	5.201
Min rZ	62	31.2DL+1.6L	2.097	-4.578	0.143	5.038
Max Rst	587	31.2DL+1.6L	0.425	-12.079	1.191	**12.145**

FIGURE 18. Deflection Shape and maximum deflection results of RD#3, having in plan theta angle 22.5° and rings spacing 1.5 m

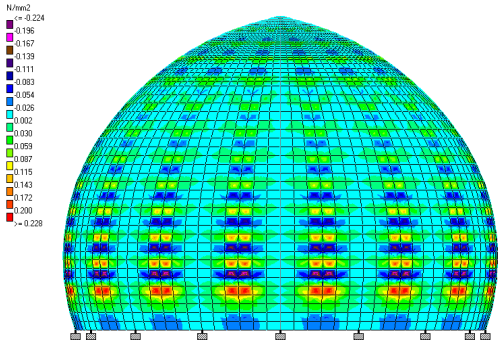

FIGURE 19. Hoop Stresses of RD#3, having in plan theta angle 22.5° and rings spacing 1.5 m

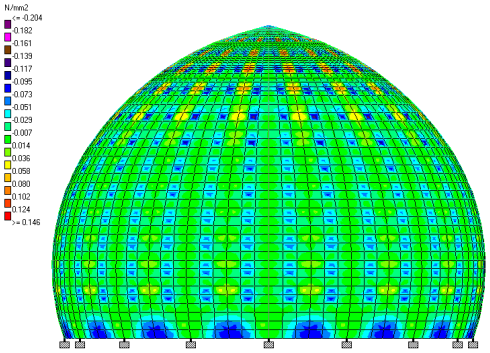

FIGURE 20. Meridional Stresses of RD#3, having in plan theta angle 22.5° and rings spacing 1.5 m

All / Summary

	Node	L/C	Horizontal X mm	Vertical Y mm	Horizontal Z mm	Resultant mm
Min X	3146	31.2DL+1.6L	**-5.937**	-3.743	-0.971	7.065
Max Y	1	31.2DL+1.6L	-0.000	**-0.000**	-0.000	0.000
Min Y	6741	31.2DL+1.6L	0.197	**-13.077**	1.244	13.138
Max Z	4178	31.2DL+1.6L	-0.969	-3.756	**6.003**	7.147
Min Z	2114	31.2DL+1.6L	1.048	-3.744	**-5.943**	7.102
Max rX	1254	31.2DL+1.6L	-0.847	-5.747	4.123	7.123
Min rX	630	31.2DL+1.6L	0.932	-5.730	-4.046	7.076
Max rY	1468	31.2DL+1.6L	3.482	-5.820	2.451	7.211
Min rY	345	31.2DL+1.6L	4.184	-5.816	-0.418	7.177
Max rZ	942	31.2DL+1.6L	-4.041	-5.731	-0.848	7.064
Min rZ	65	31.2DL+1.6L	3.838	-5.988	0.905	7.170
Max Rst	6966	31.2DL+1.6L	0.589	-13.074	1.153	**13.138**

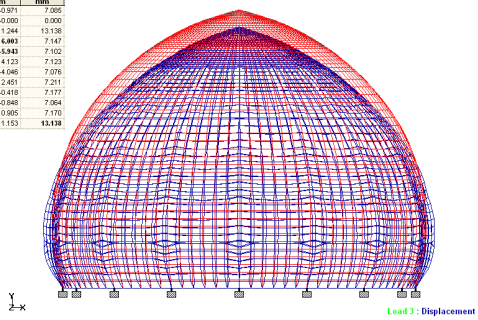

FIGURE 21. Deflection Shape and maximum deflection results of RD#4, having in plan theta angle 22.5° and rings spacing 3.0 m

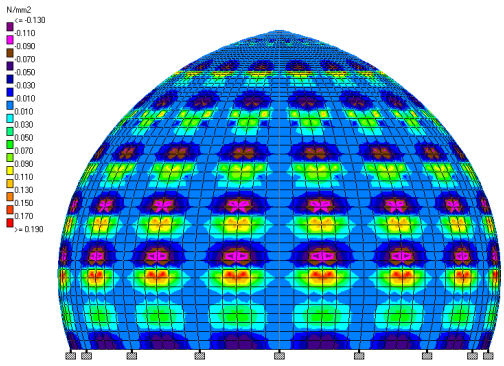

FIGURE 22. Hoop Stresses of RD#4, having in plan theta angle 22.5° and rings spacing 3.0 m

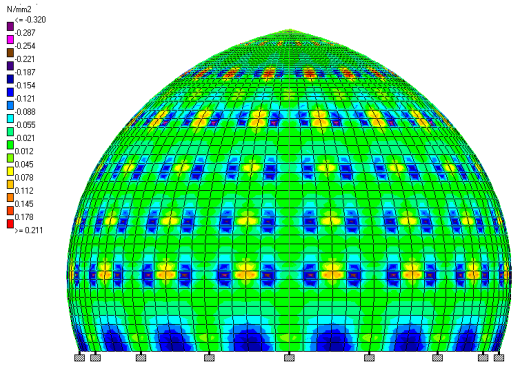

FIGURE 23. Meridional Stresses of RD#4, having in plan theta angle 22.5° and rings spacing 3.0 m

All / Summary

	Node	L/C	Horizontal X mm	Vertical Y mm	Horizontal Z mm	Resultant mm
Min Y	7366	31.2DL+1.6L	-0.476	**-12.989**	-0.474	13.007
Max Z	4154	31.2DL+1.6L	1.169	-4.198	**5.089**	6.700
Min Z	1466	31.2DL+1.6L	-1.169	-4.198	**-5.089**	6.700
Max rX	3872	31.2DL+1.6L	-0.949	-5.709	3.244	6.635
Min rX	1184	31.2DL+1.6L	0.949	-5.709	-3.244	6.635
Max rY	5401	31.2DL+1.6L	3.100	-6.694	0.989	7.443
Min rY	4272	31.2DL+1.6L	0.575	-6.684	3.181	7.425
Max rZ	2528	31.2DL+1.6L	-3.244	-5.709	-0.949	6.635
Min rZ	5216	31.2DL+1.6L	3.244	-5.709	0.949	6.635
Max Rst	7366	31.2DL+1.6L	-0.476	-12.989	-0.474	**13.007**

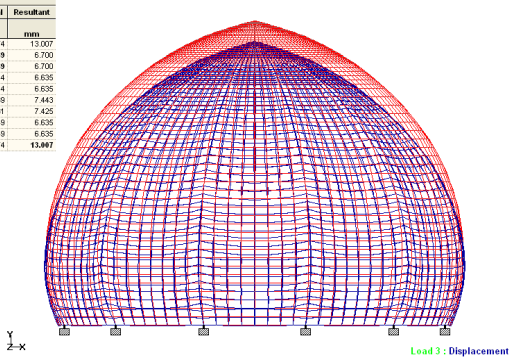

FIGURE 24. Deflection Shape and maximum deflection results of RD#5, having in plan theta angle 30° and rings spacing 1.5 m

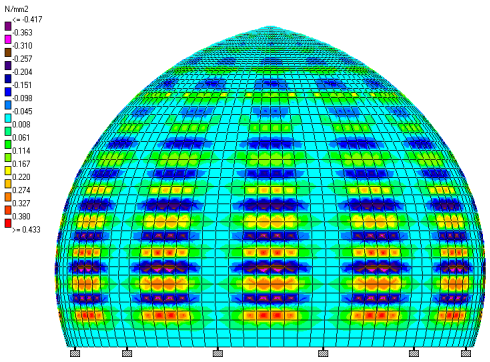

FIGURE 25. Hoop Stresses of RD#5, having in plan theta angle 30° and rings spacing 1.5 m

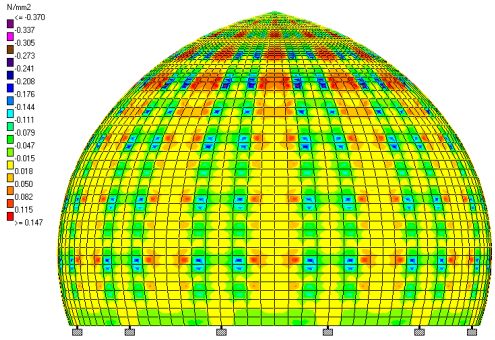

FIGURE 26. Meridional Stresses of RD#5, having in plan theta angle 30° and rings spacing 1.5 m

All \ Summary /

	Node	L/C	Horizontal X mm	Vertical Y mm	Horizontal Z mm	Resultant mm
Max X	10	31 2DL+1.6L	**5.084**	-4.453	0.714	6.795
Min X	2587	31 2DL+1.6L	**-5.084**	-4.453	-0.714	6.795
Max Y	786	31 2DL+1.6L	-0.000	**-0.000**	0.000	0.000
Min Y	5753	31 2DL+1.6L	-1.629	**-13.430**	-0.652	13.544
Max Z	3931	31 2DL+1.6L	-0.714	-4.453	**5.084**	6.795
Min Z	1243	31 2DL+1.6L	0.714	-4.453	**-5.084**	6.795
Max rX	4096	31 2DL+1.6L	-0.508	-5.620	2.867	6.329
Min rX	1408	31 2DL+1.6L	0.508	-5.620	-2.867	6.329
Max rY	5436	31 2DL+1.6L	3.430	-6.059	0.269	6.968
Min rY	5686	31 2DL+1.6L	3.612	-6.048	-0.360	7.054
Max rZ	2752	31 2DL+1.6L	-2.867	-5.620	-0.508	6.329
Min rZ	64	31 2DL+1.6L	2.867	-5.620	0.508	6.329
Max Rst	6803	31 2DL+1.6L	-0.652	-13.430	1.629	**13.544**

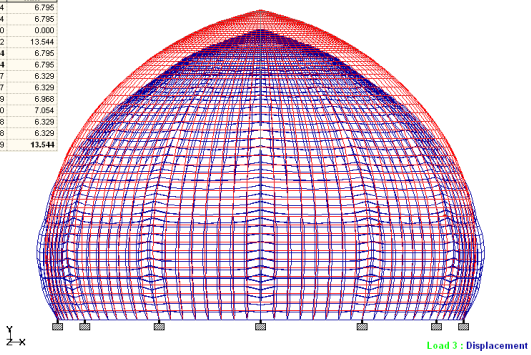

FIGURE 27. Deflection Shape and maximum deflection results of RD#6, having in plan theta angle 30° and rings spacing 3.0 m

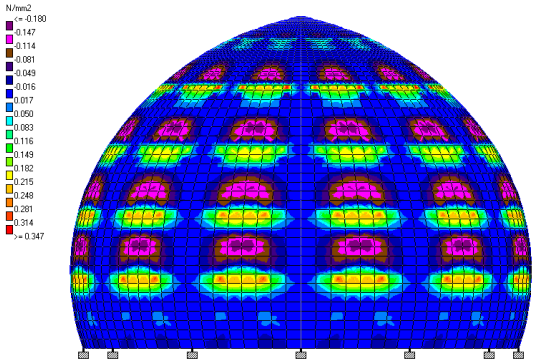

FIGURE 28. Hoop Stresses of RD#6, having in plan theta angle 30° and rings spacing 3.0 m

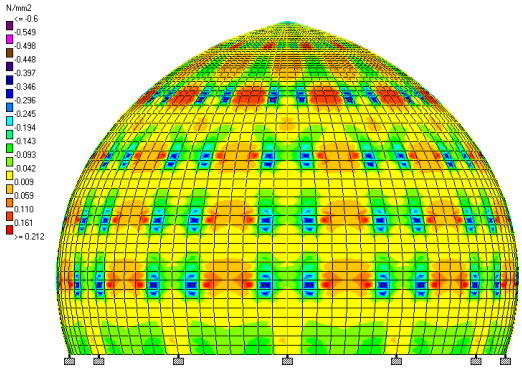

FIGURE 29. Meridional Stresses of RD#6, having in plan theta angle 30° and rings spacing 3.0 m

TABLE 2. Comparing size of member, deflections, and maximum stresses in various cases of dome

Dome case description		Size of member B.S.	Max. tension hoop stress (MPa)	Max. compression hoop stress (MPa)	Max. compression meridional stress (MPa)	Max. tension meridional stress (MPa)	Max. vertical deflection near crown (mm)	Max. horizontal deflection at springing (mm)
Brick dome (BD#1)	240 mm Thick.	-	0.60	-0.34	-0.60	-	1.47	0.91
Brick dome (BD#2)	600 mm Thick.	-	0.38	-0.30	-0.47	-	1.12	0.61
Brick dome (BD#3)	600-240 mm Thick.	-	0.24	-0.20	-0.30	-	0.99	0.38
Ribbed dome #1 (RD#1)	Rib	UB 305x165x40	0.08	-0.05	-0.20	-	10.0	3.3
	Ring	Double CH. 180x90x26						
Ribbed dome #2 (RD#2)	Rib	UB 254x146x37	0.13	-0.06	-0.33	-	10.7	4.8
	Ring	Double CH. 300x100x46						
Ribbed dome #3 (RD#3)	Rib	UB 254x146x31	0.22	-0.22	-0.21	0.13	12.1	4.6
	Ring	Double CH. 180x75x20						
Ribbed dome #4 (RD#4)	Rib	UB 203x133x30	0.19	-0.13	-0.32	0.20	13.1	6.0
	Ring	Double CH. 150x90x24						
Ribbed dome #5 (RD#5)	Rib	UB 305x165x40	0.43	-0.41	-0.37	0.14	13.0	5.1
	Ring	Double CH. 180x90x26						
Ribbed dome #6 (RD#6)	Rib	UB 254x146x37	0.34	-0.18	-0.6	0.20	13.4	5.1
	Ring	Double CH. 300x100x46						

RESULTS OF STRESSES

A compression stresses are typically much lower than crushing strength in masonry structures. As a result, crushing is not a common mode of failure for masonry structures. Furthermore, tension stresses, including shear stresses, reach tension strength in a variety of locations. As a result, masonry cracking is a common occurrence. As a result of the higher loads, masonry cracks and tension stresses become redundant [9].

Figures 4, 7 and 10 were showed the hoop stresses of brick domes under the dead and live load combination. Inspection of the figures reveals that the tension hoop stresses increase almost linearly, and the maximum value are reach near the base of dome at angle of embrace (vertical angle) phi ϕ 90 degrees, whereas various stress concentration can be seen at the same region along circumference of the dome which may explain why various of local meridional cracks exist at these places.

The analysis revealed that brick domes with constant brick thicknesses of 240 mm and 600 mm could not successfully resist the applied loads because the hoop tensile stress near the bottom region (springing region) is 0.60 MPa and 0.38 MPa, which is greater than the brick tensile strength of 0.2 MPa, while the compressive stresses were less than the allowable compressive strength. Furthermore, the results show that the good behavior of the stepped dome has a maximum tensile stress that is close to the magnitude of the tensile strength of brick, with less compressive stress. On the other hand, the deflections were very small especially for stepped brick dome as compared with ribbed dome results.

In order to compare the brick dome with ribbed dome, new analysis of the same dimensions of brick dome were done. Standards steel section was used for ribs and rings, 240 mm thickness of brick fill the area between ribs and rings. The behavior of this dome under the same load was study

The analysis showed, that the dome with steel ribs of angle in plan theta (15) were successful to resist the loads and the hoop tensile stresses of brick were less than 0.2MPa (maximum tensile strength of used brick), a meridional stress were compression stresses in the whole areas and the values less than the permissible compressive stresses 0.8 MPa. Also, the results exhibit that when the spacing between rings decrease, the hoop stresses decrease accordingly.

In case of ribbed dome with angle in plan theta (22.5 Degree) and spacing between rings were 1.5 m, tension and compression stresses appear in some regions of the meridional direction, the value of hoop tensile stress was greater than the meridional tensile stress. This is because of local buckling in the closed steel ring beams which press on the brick and cause indirect tension in brick (hoop tension stresses). When the spacing between steel ring beam increases to 3 m, opposite behavior observed. In this case meridional tensile stress was greater than the hoop tensile stress. This is occurring because of large distance between rings produce large span of ribs, therefore local buckling in ribs which compress the infill surface of brick. This led to high meridional tension stresses.

According to the above behavior of ribbed dome, the distribution of ribs and rings need to make an optimization to obtain a safe design of ribbed dome and to decrease the stresses on brick.

Similar behavior of ribbed with angle in plane theta (22.5 Degree) was observed for ribbed dome of angle in plane theta (30 Degree) and spacing between rings 1.5 m and 3 m. While the hoop tensile stress exceeds the maximum tensile strength of brick, because of great span of rings.

By deviating away from the median radius of the dome's thrust line, axial forces create a moment that causes structural deflection, which creates tensile stresses owing to deflection in the structure and results in the hinge seen in Figure 30, [15]. dome is separated into arches by ribs and rings, similar to a single-layer latticed shell's arch (a single-layer latticed shell is a structural system with rigid joints). Shells with broad spans can resist axial forces as well as internal moments and torsions. Single-layer lattice shells can buckle; hence the span should be kept as short as feasible [4].

In addition, local buckling may occur in some joints of ribbed domes because of the tiny ratio of t/R (t is the equivalent shell thickness and R the radius of curvature) Local buckling of single-layer latticed shells is also a problem. Nevertheless, the mechanism of interlocking and friction between the bricks and mortar with ribs and rings allows masonry to transmit considerable tension stresses owing to buckling of steel ribs and rings. The preceding behavior is explained why the meridional stresses in bricks between ribs and rings of large spans segments may be suffered from tension stress instead of compression in some locations of ribbed dome, See Figures 20, 23, 26, and 29 that show the producing tension meridian stress in some locations of ribbed dome.

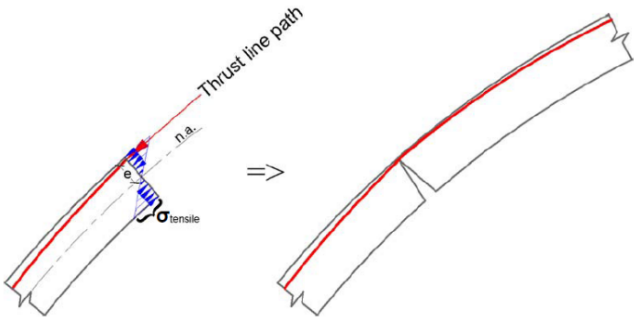

FIGURE 30. Eccentricity of the thrust line location with respect to the dome section's neutral axis [15]

RESULTS OF DEFLECTION

Domes must be evaluated for stability and safety due to deflection, a major deformation. Joint instability of a dome structure can occur if one joint in the dome exhibits significant displacement when compared to other joints. Due to stiff joints, local instabilities can be prevented. Table 2 gives the maximum deflection occurred in the domes structure representing by STAAD Pro. software, brick dome especially stepped type shows smaller deflection than ribbed domes, because the effect of surface element of brick work as shell of revolution which controlling deflection of structure due to its membrane action, Table 2 and Figures 6, 9 and 12 have been illustrated that the small magnitude of horizontal deflection occurs at the critical springing region, angle of embrace (vertical angle) phi (ϕ) 90 degree, the values are (0.91, 0.61 and 0.38) mm outward of brick dome BD#1, BD#2 and BD#3 respectively. Effect of plate element in ribbed dome are small because the release in the flow of stresses occur between the brick and steel ribs and rings in spite of producing of lateral bracing for ribs by brick, therefore the deflection of structure is more as shown in Table 2. Figures 12, 15, 16, 21, 24, and 27 are show that the maximum horizontal deflection occurs at steel ribs around the region of springing, angle of embrace (vertical angle) phi (ϕ) 90 degree, the maximum horizontal deflection magnitude range from 3.3 to 6.0 mm outward of dome, this behavior may cause cracks and crush the finishing works.

CONCLUSIONS

- Brick dome shows well performance of deflection especially stepped brick dome, the deflection was much smaller than that of comparing ribbed domes, due to its structural rigidity, that's because of its rigidity, which causes it to become unstable when the load increases and surpasses the ultimate load. Rather than ribbed domes are exhibit much vertical and horizontal deflection due to joint displacement of steel sections of ribs and rings in spite of significance effect of surface element of filled bricks in control of deflection within the permissible limits. This behavior may lead to relative movement between steel sections and it's beside bricks, and then produces cracks in junction regions of bricks with ribs.
- A comparison of the results, masonry (brick) domes with constant thickness 240 mm and 600 mm have maximum tension hoop stress (0.60 and 0.38) MPa respectively, it was greater than the limits of tensile strength in brick class B (0.20) MPa, also greater the maximum tension stress in ribbed domes. So that the cracks will be induced in a springing region. While stepped brick dome has maximum tension hoop stress (0.24) MPa and it was closed value to the limits of tensile strength in brick class B (0.20) MPa, and smaller than hoop tension stress in particular ribbed domes.
- Compressive stresses of the brick dome, and ribbed dome were lower than masonry compressive strength (0.80) MPa. Thus, crushing is not a significant mode of failure for studied domes.
- The ribbed dome, having in plan theta angle 15^{o} revealed better performance against external loads such that distribution of deformations and principal tension stresses are restricted to a limited brick surface area, since the stresses are much smaller than the allowable values, the dome is stable and have too strong capacity against common combined loadings. While in the ribbed dome, having in plan theta angle 22.5^{o} and 30^{o} the maximum

values of deformations and tension stresses in brick surface are larger and spread out near the whole of the surface, therefore the stresses are greater than the maximum allowable tension stress.

- The design of domes is needing a well control for the thickness of brick considering increase thickness in critical regions to minimize the stress and decrease the thickness at the top region to lower dead load. Relating to ribbed domes distribution of ribs and rings to obtain a safe structural system and to decrease the stresses on brick, by decreasing the value of in plan theta angle, less than or equal to (15 Degree) for this critical geometry of domes.

REFERENCES

1. S. E. Baldwin, "The dome: A study in the History of Ideas" (Princeton, New Jersey, 1971).
2. J. Heyman, "The Stone skeleton" (1st ed. New York: Cambridge University Press. 1995).
3. Ch. Peter, V. S. Dipu, P. M Manju, IJERA, ISSN:2248-9622, 25-32 (2014).
4. Ch. Wai-Fah, M. L. Eric, " Hand Book of Structural Engineering" (Taylor and Francis Group, 2005).
5. C. B. Ronaldo, S. P. Miche'le, M. B. Eduardo, J. Constr. Steel Res. **57**, 15-28 (2001).
6. D. P. Abrams, "Strength and Behavior of Unreinforced Masonry Elements" (Proceedings of 10th world conference on earthquake Engineering, Madrid, Spain, July 19 – July 24, 1992), pp. 3475-3480.
7. S.Tringali, R. De Benedictis, C. Gavarini, and R. La Rosa, " The cathedral of Noto: from the Analysis of the Collapse to the Restoration and Reconstruction Project" (Proceedings of the UNESCO/ICOMOS International Mellennium Congress Archi 2000, Paris, France, September 10 – September 12, 2001).
8. J. Heyman, Int. J. Solids Struct. 227-241 (1967).
9. Z. Nanhai, Y. Jihong, J. Eng. Mech. ASCE. **140**, 112-127 (2014).
10. C. Blasi, P. Foraboschi, J. Struct. Eng. ASCE. **120**, 2288- 2309 (1994).
11. Iraqi Standards No.25/1988, “Clayey Building Bricks” (Ministry of Housing and Construction, Baghdad, 2004).
12. B.S. 4: Part 1, “Structural steel sections, part 1. Specification for hot-rolled sections”, (1993).
13. Uniform Building Code. 2, (1997).
14. American Society of Civil Engineers ASCE/ SEI 7 - 05, " Minimum Design Loads for Buildings and Other Structures", (Reston, Virginia, 2006).
15. W. L. Wanda," Equilibrium Analysis of Masonry Domes" (M.Sc. Thesis, Massachusetts institute of technology, 2006).